Jurnal Kejuruteraan 38(4) 2026: 1773-1783
https://doi.org/10.17576/jkukm-2026-38(4)-18

CFD and Tomography-Based Analysis of Sand-Induced Erosion in Oil Flow Through a Double-Bend Pipeline

Nur Tantiyani Ali Othman* & Nurul Syifaa Nordin

Department of Chemical and Process Engineering, Faculty of Engineering & Built Environment, Universiti Kebangsaan Malaysia, 43600, Selangor Malaysia

**Corresponding author: tantiyani@ukm.edu.my*

Received 22 December 2025, Received in revised form 29 April 2026
Accepted 29 May 2026, Available online 30 July 2026

ABSTRACT

This study investigates erosion behaviour within a double-bend piping configuration subjected to sand-laden multiphase flow using Computational Fluid Dynamics (CFD). Three erosion prediction models E/CRC, Finnie, and DNV were applied to quantify erosion rate under varying particle diameters, inlet velocities, and sand concentrations. Simulations were conducted for particle diameters ranging from 100-250 µm, inlet velocities between 2-5 m/s, and sand mass flow rates of 30-90 g/s. The results show a strong dependence of erosion rate on particle inertia, impact angle distribution, and secondary flow structures (Dean vortices) generated within the bends. Statistical analyses based on standard deviation and coefficient of variation were employed to quantify moderate-to-strong variability in predicted erosion rates across operating conditions, with the E/CRC model producing a mean erosion rate of 0.00252 kg/m²·s. The first bend consistently exhibits 1.46 times higher erosion due to concentrated particle impingement at shallow to moderate angles. The study highlights optimal erosion inducing conditions at medium particle sizes and moderate-to-high inlet velocities. These findings provide a mechanistic and quantitative basis for improved pipeline design and erosion mitigation strategies.

Keywords: Sand erosion; multiphase flow; computational fluid dynamics; Eulerian-Lagrangian modeling; oil and gas pipelines; pipeline elbow

INTRODUCTION

Erosion caused by solid particle impacts is a critical challenge in oil and gas pipeline systems, especially in multiphase transportation lines where entrained sand particles interact continuously with pipe walls. In many mature or unconsolidated reservoirs, sand production is unavoidable due to reservoir depletion, weakening of formation strength, or inadequate sand-control measures. Once transported into the pipeline network, these particles gain momentum and repeatedly strike the internal surfaces of elbows, bends, valves, tees, and other fittings, accelerating wear and surface degradation (Duan et al. 2019). Such erosion can result in gradual material thinning, leakage, impaired hydraulic performance, or even catastrophic pipeline rupture, ultimately leading to operational downtime, severe safety hazards, environmental contamination, and substantial financial losses. As a result, accurately predicting erosion behaviour has become a vital aspect of pipeline integrity management, risk assessment, and flow assurance planning, particularly in high-velocity or high-sand-loading systems.

To address this issue, numerous erosion prediction models have been developed, each embedding distinct assumptions regarding particle-wall collision physics, rebound behaviour, energy dissipation, material hardness, and the dependency of erosion rate on impact angle (Parsi et al. 2023). Among the widely applied models are the E/CRC, Finnie, and DNV models, which have demonstrated varying degrees of accuracy across different operating conditions (Finnie 1960, Zhang et al. 2007, Mousori et al. 2015 and Tebowei et al. 2016). These models differ not only in their empirical correlations and mathematical frameworks but also in the physical mechanisms they prioritise for example, ductile versus brittle erosion responses, cutting versus deformation wear, and the role of particle energy at different approach angles. Consequently, their predictions can vary significantly depending on flow regime, particle properties, wall material, and geometric complexity. When these erosion models are coupled with Computational Fluid Dynamics (CFD), a more holistic representation of the system becomes possible (Arabnejad et al. 2017). CFD allows the simultaneous resolution of multiphase flow hydrodynamics, pressure fields, particle trajectories, and turbulent structures, enabling spatially detailed mapping of erosion hotspots over intricate pipeline geometries (Adekunle et al. 2017, Wu et al. 2017 and Othman et al. 2022).

In this study, CFD is employed to investigate erosion behaviour in a double-bend pipeline configuration subjected to sand-laden multiphase flow. Double-bend systems are known to produce complex flow patterns, including secondary flows, swirling motions, and strongly asymmetric velocity distributions, all of which significantly influence particle transport and impact characteristics. These geometries are particularly prone to creating high-velocity impingement regions and recirculation zones that accelerate erosion. The present analysis examines a wide range of operational and particle conditions, with specific emphasis on: (i) the influence of inlet flow velocity, particle diameter, material hardness, and sand concentration on erosion magnitude; (ii) comparative performance, sensitivity, and contrasting predictions of the E/CRC, Finnie, and DNV erosion models under identical flow conditions; and (iii) mechanistic interpretation of erosion patterns based on particle inertia, impact angle distributions, turbulence intensity, and secondary flow structures such as Dean vortices and cross-stream migration effects. By integrating hydrodynamic insights with model-based erosion predictions, this work provides a more comprehensive understanding of erosion mechanisms in complex pipeline geometries. The findings aim to support informed decision-making in pipeline design, operational optimisation, and development of more effective erosion mitigation strategies for sand-producing oil and gas systems.

METHODOLOGY

GEOMETRY AND MESH

Figure 1 shows a 2D model of a double-bend elbow pipe geometry and the mesh structure generated on the pipe model geometry. The geometry consists of two consecutive 90° bends connected by short straight sections, forming a double-bend configuration that is representative of common pipeline layouts in offshore and onshore production systems. This arrangement is known to induce complex flow features such as secondary helical vortices, cross-stream migration, and strong velocity gradients that significantly influence particle trajectory and erosion behaviour.

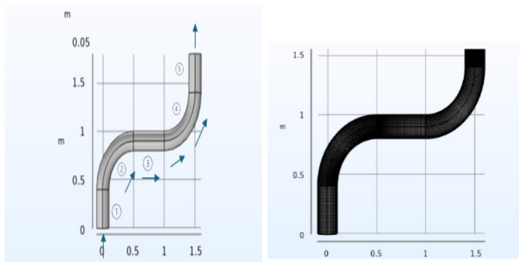

FIGURE 1. a) Double-bend elbow pipe geometry and b) Mesh structure on pipe geometry

To capture these effects accurately, a structured/unstructured hybrid mesh was generated, where structured hexahedral elements were applied in the straight pipe sections to maintain numerical stability, while unstructured tetrahedral or polyhedral elements were used in the curved bend regions to accommodate geometric complexity. Additional mesh refinement was introduced in high-gradient zones, particularly near the walls, intrados and extrados of each bend, and immediately downstream of the bend outlets where particle impingement and turbulence intensification are expected. Prism or inflation layers were incorporated adjacent to the pipe wall to resolve near-wall shear stresses and accurately compute particle-wall interactions.

Besides, mesh independence was verified through a systematic grid-convergence study involving coarse, medium, and fine grid densities. Each mesh level was evaluated based on predicted pressure drop, velocity profiles, erosion rate distribution, and particle impact frequency to ensure that the numerical solution was insensitive to further mesh refinement. Differences in key output variables between successive mesh levels were quantified using relative error metrics and Grid Convergence Index (GCI) guidelines. The final mesh selection provided an optimal balance between accuracy and computational cost, ensuring that the flow field and erosion predictions were robust and grid independent.

FLOW MODELLING

The simulations were performed using a Eulerian-Lagrangian framework. The carrier fluid phase was modelled as a continuous phase by solving the Reynoldsaveraged Navier-Stokes (RANS) equations coupled with an appropriate turbulence model. The carrier fluid was modelled as an incompressible phase using RANS equations, which provide a time-averaged representation of turbulent flow suitable for engineering-scale simulations of internal pipe flows (Tebowei et al. 2017, Salman et al. 2020, Zhang et al. 2020, Vaezi et al. 2021, Othman et al. 2022 and Parsi et al, 2023). The RANS framework is widely used in erosion modelling because it offers a good balance between accuracy and computational efficiency, especially when predicting flow patterns in complex geometries such as bends and elbows. Sand particles were treated as a discrete phase and tracked individually using a Lagrangian approach by integrating the particle force balance equations, which account for drag, gravity, and inertial effects. The particle-wall interactions were resolved to obtain impact velocity, impact angle, and location, which were subsequently used for erosion rate prediction.

To close the RANS equations, a validated two-equation turbulence model, either the standard k-ε or the k-ω Shear Stress Transport (SST) model was employed based on its proven reliability in capturing turbulence anisotropy, separation, and secondary flows in curved ducts (Rahman et al. 2023, Vaezi et al. 2021 and Othman et al. 2023). The k-ε model provides robustness for fully turbulent, high-Reynolds-number flows, while the k-ω SST model enhances near-wall resolution and effectively handles adverse pressure gradients typically observed in bend regions.

The turbulence closure model was selected after reviewing prior literature on CFD-based erosion prediction, where accurate representation of swirling motions, Dean vortices, and cross-stream secondary circulations is essential (Finnie 1960 and Dua et al. 2020). For improved near-wall accuracy, appropriate wall treatment strategies were incorporated either standard wall functions for k-ε or low-Re formulations for k-ω SST ensuring reliable prediction of velocity gradients and shear stresses that directly influence particle trajectories and impact angles (Rahman et al. 2023 and Othman et al. 2024). The incompressible assumption for the carrier fluid (typically oil, gas-liquid mixture, or water) was justified by the relatively low Mach numbers and minimal density variation across the domain.

Transport equations for turbulent kinetic energy (k) and specific dissipation rate (ω) or turbulence dissipation (ε) were solved alongside the momentum and continuity equations to capture turbulence production mechanisms induced by curvature and velocity redistribution within the double-bend configuration. These formulations allowed the model to reproduce the strong secondary flows and high swirling intensities generated within the bends, which are critical for accurately determining particle-wall interactions and the resulting erosion behaviour. Overall, the combined RANS-turbulence closure approach provided a computationally efficient yet physically reliable basis for resolving the hydrodynamic structures governing erosion in sand-laden multiphase flows.

PARTICLE TRACKING AND EROSION MODELS

Lagrangian particle tracking was employed to model the motion of sand particles suspended in the carrier fluid, allowing each particle to be tracked individually as it travelled through the double-bend pipeline. This approach is well-suited for erosion studies because it captures the detailed particle–wall interaction histories, including impact frequency, impact angle, rebound behaviour, and particle inertia effects. Sand particles with diameters ranging from 75-250 μm were considered, representing typical sizes encountered in sand-producing oil and gas wells (Othman et al. 2023). These particle sizes exhibit significant inertia relative to the surrounding fluid, making them prone to deviating from streamlines, especially within curved pipe sections where centrifugal forces and secondary flows dominate. The discrete phase motion was governed by Newton's second law, accounting for drag, lift, pressure gradient forces, and turbulent dispersion through a stochastic eddy-interaction model. Particle-wall collisions were modelled using restitution coefficients and angular momentum considerations to predict both rebound trajectories and energy losses.

BOUNDARY CONDITIONS AND OPERATING PARAMETERS

Simulations were conducted across a range of inlet velocities between 1-5 m/s, representing typical operating conditions for multiphase transport lines in oil and gas facilities (Othman et al. 2023). These velocities were selected to capture both low-inertia particle behaviour, where particles tend to follow fluid streamlines, and high-inertia regimes, where particles exhibit substantial deviation due to centrifugal forces and turbulence-driven dispersion both of which significantly affect erosion patterns in curved pipe sections. Sand loadings were varied up to 500 ppm, covering dilute-phase concentrations commonly encountered in upstream production systems. Although the concentration is relatively low, even small amounts of sand can cause substantial erosion over time, especially in geometries with strong secondary flow structures such as double bends.

The pipe walls were treated as rigid, non-deforming boundaries, an assumption that is standard in erosion simulations where material deformation is negligible compared to the fluid-particle momentum exchange. This assumption simplifies computation while still accurately capturing erosion behaviour for metallic materials typically used in pipeline construction (e.g., carbon steel, stainless steel). No-slip velocity conditions were applied at the walls for the carrier fluid, ensuring realistic prediction of near-wall shear and flow separation. Particle-wall interaction physics were incorporated using restitution coefficients that determine the fraction of normal and tangential velocity retained after impact. These coefficients influence whether particles rebound sharply, slide along the wall, or lose significant momentum during collision.

Other physics, such as friction coefficients, collision damping, and sticking probability were treated according to standard discrete phase modelling practices. Together, these modelling choices enabled the simulations to capture realistic particle trajectories, impact frequency, energy dissipation, and erosion rate across a wide range of operating conditions. The systematic variation of inlet velocity, sand loading, particle-wall interaction parameters ensured a comprehensive understanding of how operational settings influence erosion risk within the double-bend pipeline.

MODEL COMPARISON (E/CRC, FINNIE, DNV)

The E/CRC, Finnie, and DNV models were selected due to their widespread application in ductile material erosion under turbulent multiphase flow conditions and their proven suitability for particle sizes within the 75-300 µm range. These models collectively capture cutting-dominated, deformation-dominated, and empirically calibrated erosion mechanisms relevant to oil and gas pipeline systems. Besides, the three erosion models exhibited distinct predictive behaviors due to differences in their underlying assumptions, sensitivity to flow variables, and empirical foundations. It should be noted that each erosion model has inherent limitations. The Finnie model is best suited for ductile materials and shallow impact angles but may underpredict erosion at near-normal impacts. The E/CRC model offers higher sensitivity but may overestimate localized erosion under extreme conditions. The DNV model provides conservative estimates suitable for design envelopes but may smooth localized hotspots. Therefore, model selection should align with the intended engineering objective.

E/CRC MODEL

The Erosion/Corrosion Research Center (E/CRC) model produced moderate-to-high erosion rates, particularly in regions where particles experienced high-impact velocities and significant normal components of momentum (Zhang et al. 2007). One of the key characteristics of this model is its strong sensitivity to particle diameter, as larger particles possess greater inertia and therefore impart higher kinetic energy during wall impacts. The model's formulation explicitly accounts for particle size, velocity, and material properties, leading to a near-quadratic increase in predicted erosion with increasing particle diameter. As a result, erosion hotspots identified by the E/CRC model typically align closely with areas of strong particle impingement, such as the extrados of the first bend and the downstream wall of the second bend. Due to its broad industrial calibration, the E/CRC model tends to provide realistic yet relatively aggressive predictions for sand-laden flow, making it suitable for risk-based design assessments.

FINNIE MODEL

The Finnie model exhibited the widest numerical spread among the three models, driven primarily by its strong dependence on impact angle distributions (Finnie 1960 and Parsi et al. 2023). Since this model was originally developed for ductile erosion dominated by micro-cutting mechanisms, it predicts maximum erosion at shallow impact angles (typically 15-30°), where particles slide or graze the surface rather than striking it perpendicularly. In regions where impact angles approach normal incidence, the Finnie model predicts significantly lower erosion compared to the other models. This makes its predictions highly variable depending on subtle changes in particle trajectories and local flow patterns. Consequently, the Finnie model often identifies erosion hotspots at wall locations where glancing impacts dominate, such as upstream of bend entrances or along the outer curvature where particle slip occurs. But it may underpredict erosion in high-angle, high energy impact zones, potentially making it less conservative for design purposes under certain flow and geometry conditions.

DNV MODEL

The DNV model produced more conservative and uniformly distributed erosion predictions, reflecting its basis in empirical datasets compiled for offshore industry applications (Parsi et al. 2023 and Zhang et al. 2007). Unlike the Finnie model, the DNV formulation is not strongly angle-dependent and incorporates impact velocity, particle mass, and material hardness in a way that tends to smooth out extreme variations in erosion rate. As a result, erosion patterns predicted by the DNV model are more spatially uniform, with moderate peaks that remain within a narrow range even when flow velocity or particle size increases. This stability makes the DNV model attractive for design control and regulatory compliance, as it avoids excessive sensitivity to small fluctuations in flow conditions. While the DNV model may slightly underestimate highly localized erosion hotspots, it provides a balanced and industry validated assessment suitable for engineering design envelopes.

MECHANISTIC INTERPRETATION

Erosion in this configuration is governed by three primary mechanisms: particle inertia which causes particles to overshoot curvature and strike walls with high momentum, secondary flow effects where Dean vortices redirect particles into concentrated attack zones and the impact angles where cutting-dominated angles generate high erosion at shallow-to-moderate incidence. These mechanisms explain the dominance of erosion in the first bend and the observed dependence on particle size and velocity.

MODEL COMPARISON

Although no dedicated experimental work was conducted in the present study, the predicted erosion magnitudes and spatial distributions were benchmarked against well-documented experimental and numerical studies reported in the literature. For comparable elbow geometries and sand-laden flow conditions, Mansouri et al. (2015), Zhang et al. (2007), and Parsi et al. (2023) reported erosion rates in the order of 10^{-3}-10^{-2} kg/m²·s, which are consistent with the present predictions obtained using the Finnie, DNV, and E/CRC models. Besides, the dominance of erosion at the extrados of the first bend and the sensitivity to particle size and velocity closely match experimentally observed erosion patterns, providing confidence in the validity of the adopted CFD-erosion modelling framework.

RESULTS & DISCUSSION

Figure 2 displays the surface pressure distribution and wall resolution in the two-phase pipeline system involving crude oil and solid particles as simulated using COMSOL Multiphysics®. The pressure scale ranges from approximately -4×10^4 Pa to 9×10^4 Pa. Red areas indicate regions of highest pressure, while light blue to purple shades represents the lowest pressure zones in the pipe domain. For the wall resolution values range from 0.1 to 0.9, with blue indicating the lowest values and red representing the highest. Based on the colour scale and distribution, it is evident that regions near the curved wall sections and the middle of the horizontal pipe exhibit higher wall resolution values (from red to orange), whereas other regions such as the inlet and outlet sections show lower resolution (from green to blue).

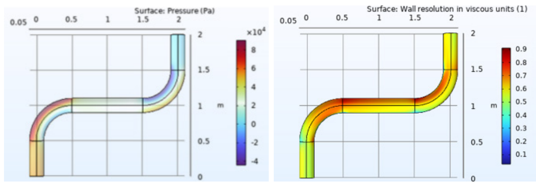

(a) (b)

FIGURE 2. a) Pressure distribution and b) Wall resolution

TEMPORAL EVOLUTION OF PARTICLE TRAJECTORIES

The implementation of the Lagrangian particle tracking method is illustrated through particle trajectory distributions and erosion contours along the double-bend geometry. The predicted erosion hotspots correspond to regions of high particle impingement frequency and elevated impact velocities. Figure 3 illustrates the trajectory of sand particles within two-phase pipeline system at t=0.055 - 0.135 s. The presence of secondary flow structures, such as Dean vortices induced by pipe curvature, influences particle migration towards the outer wall of the bends, thereby intensifying local erosion. Although instantaneous vortex scratching is not resolved in the RANS framework, the time-averaged effects of turbulent secondary flows on particle dynamics are adequately captured through the Lagrangian approach. As the flow enters the first bend, these vortices intensify and form a strong pair of counter-rotating motions that drive particles toward outer wall. This results in the development of localized particle-focusing zones, where particle-wall interactions become more frequent and energetic.

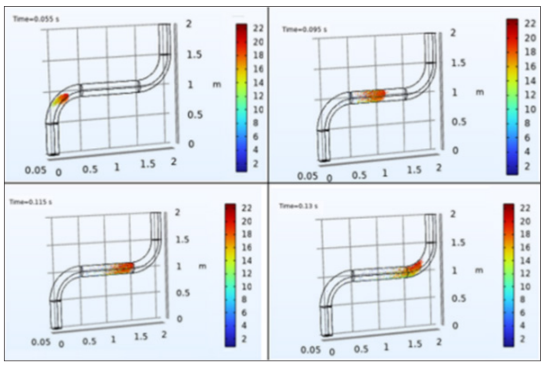

FIGURE 3. Visualization of sand particle trajectories in the pipeline system at various time steps (t=0.055 s, 0.095 s, 0.115 s, 0.135 s)

By contrast, the strength of the secondary motion diminishes substantially in the second bend, largely due to prior momentum dissipation and partial particle redistribution occurring downstream of Bend 1. Consequently, erosion levels in Bend 2 are significantly lower, as the weakened vortices are less capable of directing particles forcefully toward the walls. Particle behaviour is also strongly influenced by inertial lag, particularly at higher flow velocities and with larger particle diameters. Under these conditions, particles diverge from fluid streamlines and impact outer curvature with greater momentum. Notably, medium sized particles (100-170 µm) emerge as most effective erosive agents. Their size provides an optimal balance between maintaining sufficient inertia and retaining sensitivity to the redirection imposed by Dean vortices, resulting in the highest probability of wall impact.

The transient particle-tracking results provide detailed insight into how erosion hotspots develop over time. At *t*=0.055 s, particles enter the pipeline from the bottom, traveling in a nearly linear trajectory aligned with the main flow. No accumulation occurs at this stage since the particles have not yet reached the bend region. At *t*=0.095 s, particles begin to encounter the curved geometry. Centrifugal effects become dominant, causing particles to migrate outward and concentrate along the bend's external wall. This motion reflects the combined influence of curvature-induced pressure gradients and particle inertia.

At *t*=0.115 s, large particle accumulation forms near the outer curvature. Particles begin to impact the wall at a range of angles, producing localized regions of elevated kinetic energy. High-velocity particles (indicated by red in the velocity contours) contribute disproportionately to material removal. At *t*=0.135 s, most particles exit the bend and move upward into the vertical pipe section. Yet, some particles remain trapped or recirculate near the outer wall, indicating a region of persistent erosion risk due to repeated particle surface interactions. These dynamic patterns provide critical operational insights for industries such as oil and gas, where sand-laden multiphase flow routinely damages elbows, tees, and other geometric transitions. Recognizing these high-risk trajectories allows for targeted use of erosion-resistant liners, optimized bend geometries, or flow-conditioning devices to extend pipeline service life.

MAXIMUM EROSION RATE AND PARAMETRIC INFLUENCE

There are about 40 simulation cases performed to evaluate how variations in inlet fluid velocity, particle diameter, and sand mass flow rate influence the maximum erosion rate in a two-phase flow environment. All simulations used a steady-state Eulerian-Lagrangian framework, and erosion predictions were derived using three established models: E/CRC, Finnie, and DNV. Although the pipeline geometry and boundary conditions were held constant, systematic parameter variations revealed several important trends.

EFFECT OF FLUID VELOCITY

Figure 4 illustrates the relationship between fluid velocity; 2 -5 m/s and maximum erosion rate predicted by the E/CRC model for particles of three sizes. The results show a marked increase in erosion rate with increasing velocity, consistent with theoretical expectations: higher flow velocities impart greater kinetic energy to particles, intensifying their impact forces on the pipe wall (Wang et al. 2025).

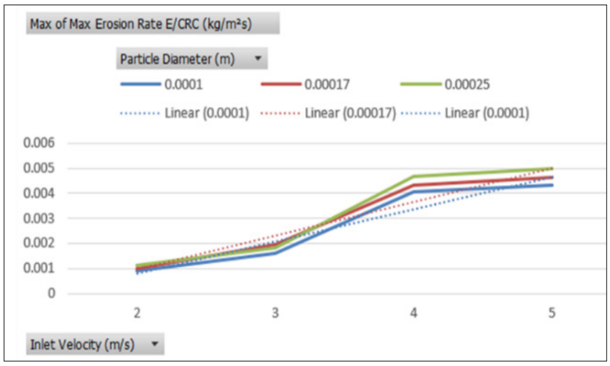

FIGURE 4. Effect of Fluid Velocity on Erosion Rate

Across all velocities, erosion rates follow the order of 250 µm > 170 µm > 100 µm. This trend is governed by inertia, where larger, heavier particles experience weaker drag deceleration and thus retain higher momentum on impact. Previous studies have shown erosion diameter relationships can sometimes be non-monotonic, depending on pressure, temperature, or particle morphology (Zhang et al. 2007, Othman et al. 2023 and Wang et al. 2025). Still, in the diameter range considered here (100-250 µm), the simulation results reveal a consistent rise in erosion rate with diameter, confirming the strong coupled influence of fluid velocity and particle size on erosion rate in multiphase pipe systems. As well, increased fluid velocity (4-5 m/s) consistently led to higher erosion rates. This relationship is attributed to the greater kinetic energy imparted to particles, resulting in more energetic and damaging impacts on pipe surfaces.

EFFECT OF PARTICLE DIAMETER AND MOMENTUM

Figure 5 depicts the variation of maximum erosion rate with particle diameter for four different fluid velocities. For all velocities, erosion increases steadily as particle diameter increases from 100 µm to 250 µm. Larger particles retain higher kinetic energy upon impact, making them more destructive to pipe wall surfaces.

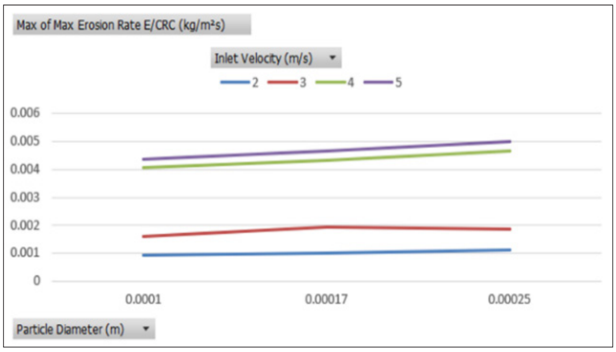

FIGURE 5. Effect of Sand Particle Diameter on Erosion Rate

The difference in erosion magnitude between particle sizes becomes more noticeable at higher velocities. At velocity of 5 m/s, the erosion rate contrast between 100 µm and 250 µm particles is significantly greater than at 2 m/s, reflecting the compounding effects of diameter and velocity on particle kinetic energy. These observations align closely with the findings of Shan et al. (2024), who reported that particle size has a stronger influence on erosion under high-velocity conditions. While some literature suggests possible non-linear trends at wider diameter ranges (Jafari et al. 2019), the monotonic increase observed in this study strongly supports diameter as a dominant parameter within the 100-250 µm range. As well larger particle sizes produced higher wall impact energies; however, excessively large particles also exhibited reduced responsiveness to secondary flow redirection. Medium-sized particles again demonstrated the highest erosive efficiency due to optimal inertia.

EFFECT OF SAND MASS FLOW RATE

Figure 6 shows the effect of sand mass flow rate on the maximum erosion rate for different particle diameters. As expected, increasing sand mass flow leads to higher erosion rates for all particle sizes. This occurs because a higher quantity of particles increases collision frequency with the pipe wall, thereby raising cumulative surface wear (Zhang et al. 2010). For any given flow rate, the erosion rate again increases with particle size, highlighting the combined effects of particle inertia and particle loading. For example, at 90 g/s, the 250 µm particles generate the highest erosion rate due to their high momentum and lower response to fluid deceleration. These findings confirm that a combination of high sand loading and large particle diameter produces the most severe erosion environment in piping systems. Also, higher sand mass flow rate did not always translate to proportionally higher erosion rates. In some cases, the increase in particle quantity caused by non-uniform particle dispersion, inter-particle collisions, and dilution of impact energy, which collectively reduced the effective erosive power per particle. These effects were reflected by the sediment retention percentages and particle counts at t=1 s.

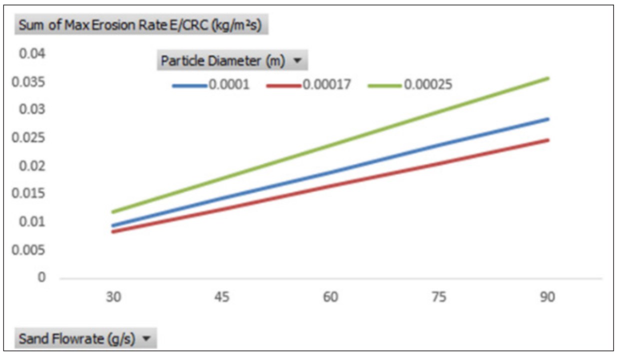

FIGURE 6. Effect of Sand Mass Flow Rate on Erosion Rate

TEMPORAL VARIATION OF EROSION RATE

Figure 7 presents the time evolution of the maximum erosion rate up to 1.5 s. The erosion rate increases rapidly during the initial 0.20 s, corresponding to the high-energy entry phase of particles into the elbow region. As particles lose momentum through wall interactions and fluid drag, the erosion rate gradually approaches a steady-state value, consistent with reported behaviour in multiphase erosion studies (Mansouri et al. 2015).

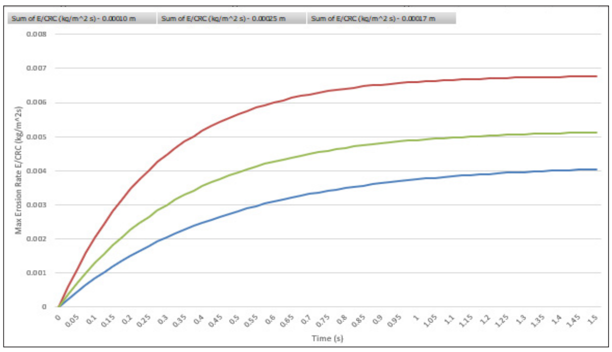

FIGURE 7. Time Evolution of The Maximum Erosion Rate Up To t=1.5 s

Interestingly, 170 µm particles show the highest erosion rates throughout the simulation period. This behaviour reflects their optimal balance of inertia and flow following ability large enough to carry significant momentum, yet small enough to respond to secondary flows that direct them into high-erosion zones. This agrees with findings by Gorji-Bandpy et al. (2014), who identified medium-sized particles as the most efficient erosive agents.

COMPARISON OF EROSION MODELS

Figure 8 compares the erosion predictions of the Finnie, E/CRC, and DNV models using the optimum conditions (5 m/s velocity, 90 g/s sand flow, 250 µm particles). The Finnie model predicts erosion concentrated in the first elbow but with a relatively low magnitude (~0.0025 kg/m²·s). This is expected because the model is based primarily on the normal impact component and does not incorporate additional empirical adjustments. Furthermore, the magnitude of 0.00252 kg/m²·s falls within the upper range of erosion rates reported for high-velocity, sand-laden elbow flows under aggressive operating conditions, as documented by Mansouri et al. (2015) and Parsi et al. (2023).

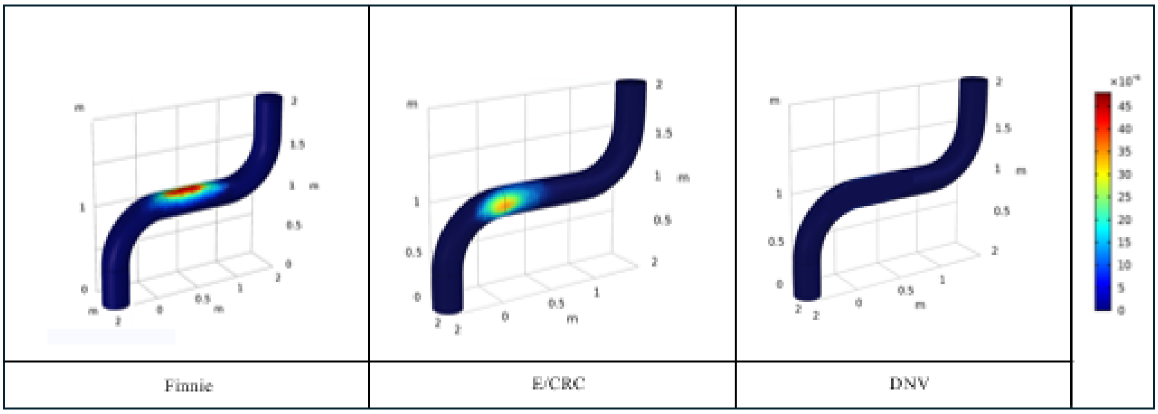

FIGURE 8. Comparison of erosion predictions based on three major empirical models: Finnie, E/CRC, and DNV

The E/CRC model produces the highest erosion values (~0.0056 kg/m²·s) and a broader erosion region due to its incorporation of multiple influencing parameters such as impact angle, particle properties, and fluid velocity. The DNV model provides the most conservative prediction (~0.0018 kg/m²·s), reflecting its intended application for long-term industrial assessments with safety margins. Figure 8 further confirms that all three models predict increasing erosion with rising fluid velocity. At 5 m/s, the E/CRC model yields a maximum erosion rate of 0.00445 kg/m²·s, significantly higher than both Finnie and DNV, emphasizing its sensitivity to operating conditions.

Overall, the selection of an erosion model should depend on the analysis objective of DNV for conservative, safety-focused assessments; Finnie for fundamental mechanistic evaluation; and E/CRC for sensitive, practical erosion prediction in real engineering conditions.

Variability in the erosion predictions was quantified using standard deviation and coefficient of variation across the parametric cases, allowing objective classification of erosion response as weak, moderate, or strong depending on operating conditions. About 40 simulation data were simulated that shows the E/CRC erosion predictions exhibit a mean value (M) of 0.00252 kg/m²·s with a standard deviation (SD) of 0.00135 kg/m²·s, while the Finnie and DNV models show similar mean levels (0.002562 kg/m²·s, 0.002195 kg/m²·s respectively) but different spreads.

SAND PARTICLE ACCUMULATION BEHAVIOUR

Figure 9 presents the accumulated distribution of sand particles with diameters of 100 µm, 170 µm, and 250 µm, accompanied by time-dependent accumulation curves beneath each distribution plot. The results demonstrate that particle size strongly influences settling behaviour, deposition rate, and transport stability within the curved pipe.

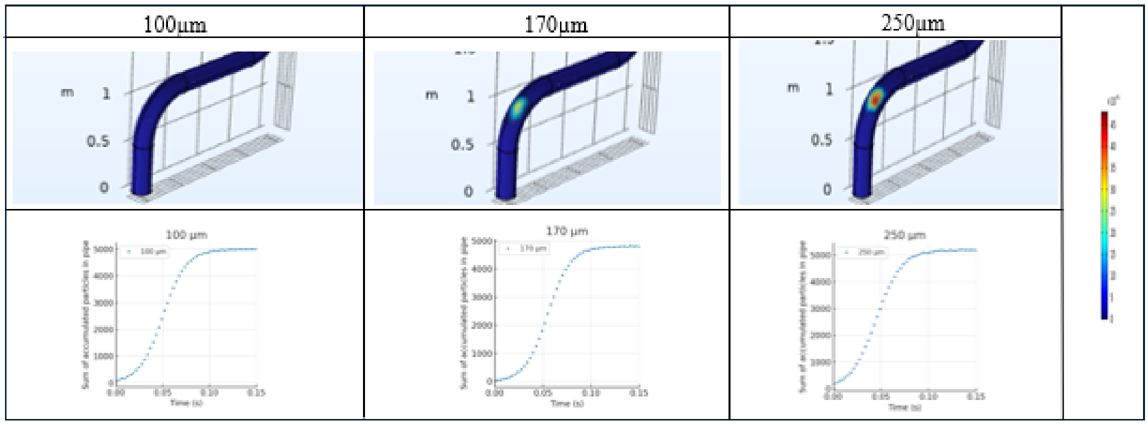

FIGURE 9. Particle Accumulation Analysis for Different Sand Diameters

For 100 µm particles, the accumulation curve exhibits a rapid rise during the early part of the simulation and then stabilizes around *t*=0.10 s. These smaller particles possess low inertia, enabling them to remain suspended within the flow for a longer duration. Their trajectories closely follow the fluid streamlines, resulting in a more uniform distribution and reduced tendency to settle along the pipe walls. This behaviour is consistent with fluid-particle transport theory, where small particles with low Stokes numbers are highly responsive to flow fluctuations and experience minimal gravitational settling.

Particles of 170 µm show a clearly different trend. Their accumulation curve indicates a sharper increase relative to the 100 µm case before reaching steady conditions. The higher inertia of these medium-sized particles allows them to partially resist fluid drag and settle more quickly, especially in low velocity recirculation regions at the inner curvature of the elbow. The results indicate a dynamic balance between particle deposition and continuous particle transport through the domain. The 250 µm particles exhibit the highest accumulation rate. Their large mass and inertia make them less influenced by the fluid flow, enabling rapid settling and formation of thicker deposition layers at the pipe bottom and downstream of the elbow. The time required to reach steady-state accumulation is shorter than for smaller particles, illustrating the strong dependence of deposition behaviour on particle inertia.

Overall, the findings clearly establish that particle diameter is a dominant factor governing accumulation dynamics. Larger particles settle faster and in greater quantities, whereas smaller particles remain suspended for longer durations. This agrees with previous studies, which report particle inertia increases with diameter, enhancing gravitational settling and reducing the influence of drag forces. These results have direct implications for erosion prediction, as zones of high accumulation are often precursors to intensified erosion.

Figure 10 shows the erosion rate analysis by evaluating particle retention at *t*=0.15 s relative to the initial particle count (5000). The percentage of remaining particles (% Remaining) and particle loss (% Loss) were quantified and grouped by operating parameters. Increasing fluid velocity consistently reduces the percentage of remaining particles, indicating greater particle–wall interactions or domain exit due to higher drag forces. Similarly, larger particle diameters exhibit lower % Remaining values, particularly at elevated velocities, due to their ballistic-like motion and reduced response to drag forces. This trend reinforces the earlier conclusion that both parameters strongly influence frequency and erosion development. Figures 4-10 explicitly support the parametric trends discussed, with each figure referenced immediately following the corresponding analysis to ensure clarity and traceability of key findings.

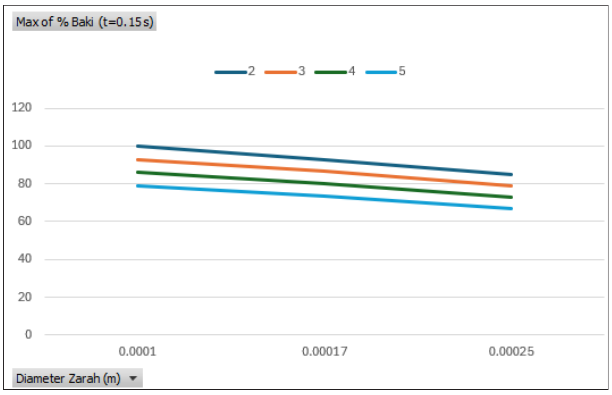

FIGURE 10. Percentage Remaining Particles at Different Particle Size in *t*=1.5 s

From an engineering perspective, the results indicate that erosion risk can be significantly reduced by increasing bend radius, limiting operating velocities below 4 m/s where feasible, and implementing sand management strategies such as upstream desanders or particle separators. Also, erosion-resistant liners or material reinforcement are recommended at the extrados of the first bend, which consistently experiences the highest erosion rate. These design and operational measures directly support safer pipeline operation and extended service life.

CONCLUSION

This study successfully established a high-fidelity 3D CFD framework in COMSOL Multiphysics® 6.2 to analyze sand-induced erosion in a multiphase pipeline featuring a double-bend elbow, one of the most erosion-prone geometries in the industrial systems. Across 40 simulation scenarios, including variations in flow velocity (2-5 m/s), particle diameter (100-250 µm), and sand mass flow rate (30-90 g/s), several critical erosion behaviors were identified. Erosion intensity increased up to 4 m/s before diminishing at higher velocities, demonstrating the trade-off between momentum transfer and reduced particle-wall collisions. Particle size effects were strongly non-linear, with mid-range diameters (150-200 µm) producing the most severe wear due to optimal momentum and trajectory. Conversely, higher sand mass flow rates unexpectedly lowered erosion, driven by particle shielding and near-wall sediment formation. Comparative assessment of erosion models revealed clear performance differences that the E/CRC model produced the largest erosion magnitudes and spatial spread, followed by Finnie and DNV, highlighting the sensitivity of predictions to model selection. Overall, this work not only enhances fundamental understanding of erosion mechanisms in complex pipeline geometries but also demonstrates the capability of CFD as a robust predictive tool. The insights generated offer practical guidance for optimizing pipeline design, selecting safer operating windows, and developing proactive maintenance strategies, ultimately contributing to improved reliability, reduced downtime, and extended asset life in oil and gas operations.

ACKNOWLEDGEMENT

This research is fully supported by GUP-2024-061 and FRGS grant, FRGS/1/2024/TK05/UKM/02/4. The authors fully acknowledged Ministry of Higher Education (MOHE) and Universiti Kebangsaan Malaysia for the approved fund which makes this important research viable and effective.

DECLARATION OF COMPETING INTEREST

None.

REFERENCES

Adekunle Ogunsesan, O. 2020. CFD modelling of pipe erosion under multiphase flow regimes.

Arabnejad, H., Shirazi, S. A. & McLaury, B. S. 2017. A combined CFD/experimental methodology for erosion prediction.

Duan, L., Chen, Y. & Zhang, W. 2019. Multiphase flow-induced sand erosion in oil pipelines. *Journal of Petroleum Science and Engineering* 176: 108-119.

Duan, L., Zhao, L., Wang, Z., Liu, W. & Zhou, W. 2020. Erosion characteristics of solid particles in gas-liquid pipe flow: A study using CFD simulation and experimental validation. *Chemical Engineering Science* 229: 116097.

Ejeh, C. J., Boah, E. A., Akhabue, G. P., Onyekpere, C. C., Anachuna, J. I. & Agyeibi, I. 2020. Computational fluid dynamic analysis for investigating the influence of pipe curvature on erosion rate prediction during crude oil production. *Experimental and Computational Multiphase Flow* 2(4): 255-272.

Finnie, I. 1960. Erosion of surfaces by solid particles. *Wear* 3(2): 87-103.

Gorji-Bandpy, M., Forouzi, M. A., Sadeghi, M. H. & Hosseinalipour, S. M. 2014. Numerical simulation of solid particle erosion in a 90° elbow. *Scientia Iranica*.

Jafari, H. & Hattani, M. 2019. Investigating the optimum particle size for maximum erosion in oil and gas pipelines. *Engineering Failure Analysis*.

Mansouri, A., Shirazi, S. A., McLaury, B. S., Rhyne, L. D. & Shadley, J. R. 2015. Experimental and computational study of sand erosion in elbows and plugged tees. *Journal of Energy Resources Technology*.

Othman, N. T. A. & Rostam, F. 2022. CFD modelling of sand particle transport in a horizontal multiphase 90° pipeline flow. *Journal of Engineering Science and Technology* 17(6): 4277-4290.

Othman, N. T. A., Putra, Z. A., Abidin, S. A. Z. & Ali, F. I. M. 2023. CFD analysis of erosion rate in oil and gas pipeline industry. *Jurnal Teknologi*: 59-66.

Othman, N. T. A., Putra, Z. A., Abidin, S. A. Z. & Ali, F. I. M. 2024. Integration of CFD analysis and artificial neural networks for estimation of erosion rate in oil and gas pipelines. *Results in Engineering* 24.

Parsi, M., Hajiahmadi, H. & Da Silva, M. J. 2023. CFD-based erosion prediction for multiphase flow in bends: Validation and insights. *Journal of Computational Multiphase Flow* 15(1): 41-58.

Rahman, M. M. et al. 2023. Evaluation of k-ω turbulence model in high-Reynolds number flows in curved ducts. *International Journal of Heat and Fluid Flow*.

Salman, S., Anwar, S. & Qazi, M. H. 2024. Numerical and experimental study of slug flow and erosion effects in multiphase pipelines. *Journal of Energy Resources Technology* 146(5): 052902.

Shan, X., Zhang, Y., Liu, Y. & Wang, C. 2024. CFD simulation of sand particle erosion in multiphase flow pipelines. *Powder Technology*.

Tebowei, J. 2016. Analysis of multiphase flow and erosion in oil and gas pipelines using CFD techniques. *International Journal of Energy Research* 40(10): 1356-1370.

Vaezi, S. & Mohammadi, S. 2021. Numerical simulation of multiphase flow-induced erosion in pipeline bends using CFD techniques. *Energy* 235: 121234.

Wang, Z., Li, M., Xu, J. & Zhou, Y. 2025. Effect of particle diameter on erosion-corrosion in turbulent slurry flow. *Journal of Natural Gas Science and Engineering*.

Wu, X., Zhao, H. & Liu, J. 2017. Erosion modeling in multiphase pipelines using CFD tools. *Computational Fluid Dynamics Journal* 12(3): 201-212.

Zeng, Q. & Qi, W. 2020. Simulation analysis of erosion-corrosion behaviors of elbow under gas-solid two-phase flow conditions. *Lubricants* 8(9).

Zhang, Y., McLaury, B. S. & Shirazi, S. A. 2007. A comprehensive mechanistic model for solid particle erosion in elbows and plugged tees.

Zhao, Y., Liu, Q., Zhang, T. & Zhang, Z. 2023. Impact of fluid viscosity and particle density on erosion in oil and gas pipelines. *Journal of Petroleum Science and Engineering* 222: 110111.